Stratospheric Circulation Changes Associated with the Hunga Tonga-Hunga Ha'apai Eruption

L. Coy[1,2], P. A. Newman[1], K. Wargan[1,2], G. Partyka[1,2], S. Strahan[1,3], and S. Pawson[1]

[1]NASA GSFC, Greenbelt, MD, USA.

[2]SSAI, Lanham, MD, USA.

[3]University of Maryland Baltimore County, Baltimore, MD, USA.

Corresponding author: Lawrence Coy (lawrence.coy@nasa.gov)

Key Points:

- Extreme perturbations in the stratospheric winds and temperatures are linked to a volcanic eruption.
- Hunga Tonga-Hunga Ha'apai eruption effects are unique in the stratospheric record.
- Data assimilation can track temperature and wind perturbations, even when some physics is missing.

Abstract

The 15 January 2022 eruption of the Hunga Tonga-Hunga Ha'apai underwater volcano (20.5°S, 175.4°W) injected a record amount of water directly into the stratosphere. This study attempts to quantify this impact on the temperature, as well as the subsequent changes to the stratospheric circulation, during the months following the eruption based on reanalysis fields. The extreme nature of the temperature, wind, and circulation changes are tracked through comparisons of the first six months of 2022 with the previous 42 years. Examination of the data assimilation process shows that at 20 hPa the thermal observations are forcing significant cooling, compensating for the absence of the excess stratospheric moisture in the model used for the reanalysis. In response to this cooling the atmosphere adjusts by creating strong westerly winds above the temperature anomaly and large changes to the downward and poleward mean meridional circulation.

Plain Language Summary

While the stratosphere (15-55 km) region of the atmosphere contains the ozone layer, it is typically very dry, especially when compared to the troposphere. However, the remarkable eruption of the Hunga Tonga-Hunga Ha'apai underwater volcano on 15 January 2022 injected a record amount of water directly into the stratosphere. Winds in the stratospheric soon carried this excess water vapor around the globe to all longitudes and spread the water vapor in latitude as well. Since water vapor can cool to space more rapidly than the stratospheric air, enhanced cooling in the stratosphere is expected. This study quantifies this cooling, as well as the subsequent changes to the stratospheric circulation, during the months following the eruption. The extreme nature of the stratospheric temperature, wind, and circulation changes are tracked through comparisons of the first six months of 2022 with the previous 42 years. Details of the stratospheric perturbations in latitude and pressure are presented for June 2022, where anomalously low temperatures are found at near 20 km altitude from 60°S to 30°S. In response to this cooling the atmosphere adjusts by creating strong westerly winds above the temperature anomaly and large changes to the downward and poleward mean meridional circulation.

1 Introduction

The 15 January 2022 eruption of the Hunga Tonga-Hunga Ha'apai underwater volcano (20.5°S, 175.4°W) injected an unprecedented amount of water directly into the stratosphere (Millán et al., 2022; Xu et al., 2022; Carr et al., 2022). While the initial injection plume at 20°S reached to the upper stratosphere (Carr et al., 2022), Millán et al. (2022), showed that after three months this excess water vapor settled near 20 hPa altitude in a latitude band from 30°S to 5°N. This dispersion of the water vapor in latitude is tracked by Schoeberl et al., 2022 and is generally consistent with climatological expectations. With no major thermodynamic or photochemical sinks, this excess moisture is expected to remain in the stratosphere for two to three years. Water vapor is radiatively active in the infrared, contributing to the total radiative cooling in the stratosphere, which is dominated by the effects of carbon dioxide and ozone (e.g., Gille and Lyjak, 1986). These large perturbations in water vapor are expected to increase the amount of radiation lost to space, locally cooling the stratosphere. This study attempts to quantify this impact on the temperature, as well as the subsequent changes to the stratospheric circulation, during the first six months after the eruption.

The MERRA-2 (Modern-Era Retrospective Analysis for Research and Applications, Version 2) reanalysis (Gelaro et al., 2017) provides the circulation fields (temperatures and winds) for this study. While MERRA-2 assimilates a number of in-situ and space-borne observations that constrain tropospheric moisture, stratospheric water vapor observations are not assimilated. Stratospheric moisture is closely constrained to monthly climatologies imposed by a relaxation constraint in the MERRA-2 model component, so that it does not respond to the volcanic perturbation. This precludes the use of MERRA-2 to directly infer the thermal impacts of the water vapor increase on the circulation. However, numerous nadir- and limb-sounding microwave observations are assimilated in the stratosphere (McCarty et al., 2016) and these data will constrain the analyzed temperatures, which can be used to indirectly infer the thermal and dynamical response of the stratosphere in MERRA-2. Additionally, a more recent data assimilation system, the MERRA-2 Stratospheric Composition Reanalysis of Aura Microwave Limb Sounder (M2-SCREAM : described below), does assimilate stratospheric water vapor and is used to compare with the MERRA-2 analysis and radiative temperature tendencies.

2 Assimilation Products

The 43-year (1980-2022) climate record from MERRA-2 is used to assess the anomalies of 2022. Two sets of monthly averaged files are used: The assimilation files for winds and temperatures (GMAO, 2015a), and the temperature tendency files to obtain the analysis temperature tendencies (GMAO, 2015b). The residual zonal mean circulations for each month are calculated from the monthly averaged assimilation files as, in addition to winds and temperatures, these files also contain the heat and momentum fluxes needed for evaluation of the residual circulation (see Andrews et al., 1987, page 128). For this study we examine the stream function of the residual circulation as well as the residual mean meridional and vertical winds.

M2-SCREAM (Wargan et al., 2022) is a new stratosphere-focused reanalysis product developed at NASA's Global Modeling and Assimilation Office. Temperature, winds, surface pressure, and tropospheric water vapor in M2-SCREAM are constrained by the MERRA-2 assimilated fields. M2-SCREAM assimilates stratospheric profiles of ozone, water vapor, hydrogen chloride, nitric acid, and nitrous oxide from version 4.2 retrievals of the Microwave Limb Sounder (MLS: Waters et al., 2006; Livesey et al., 2020) observations, the same as those used in Millán et al. (2022), alongside total ozone observations from the Ozone Monitoring Instrument (Levelt et al., 2006, 2018). M2-SCREAM covers the MLS period, beginning in September 2004 and presently extends to June 2022. Because MLS data are assimilated, this reanalysis represents the water vapor enhancement from the Hunga Tonga eruption. The global increase of stratospheric water vapor mass calculated from M2-SCREAM is ~10% (Fig. 1a), as in Millán et al. (2022). By June 2022 (Fig. 1b) the enhanced water vapor has spread from 60°S to 30°N. As shown below, the radiative transfer model in M2-SCREAM responds to the moisture enhancement by producing long wave cooling in better agreement with the observations.

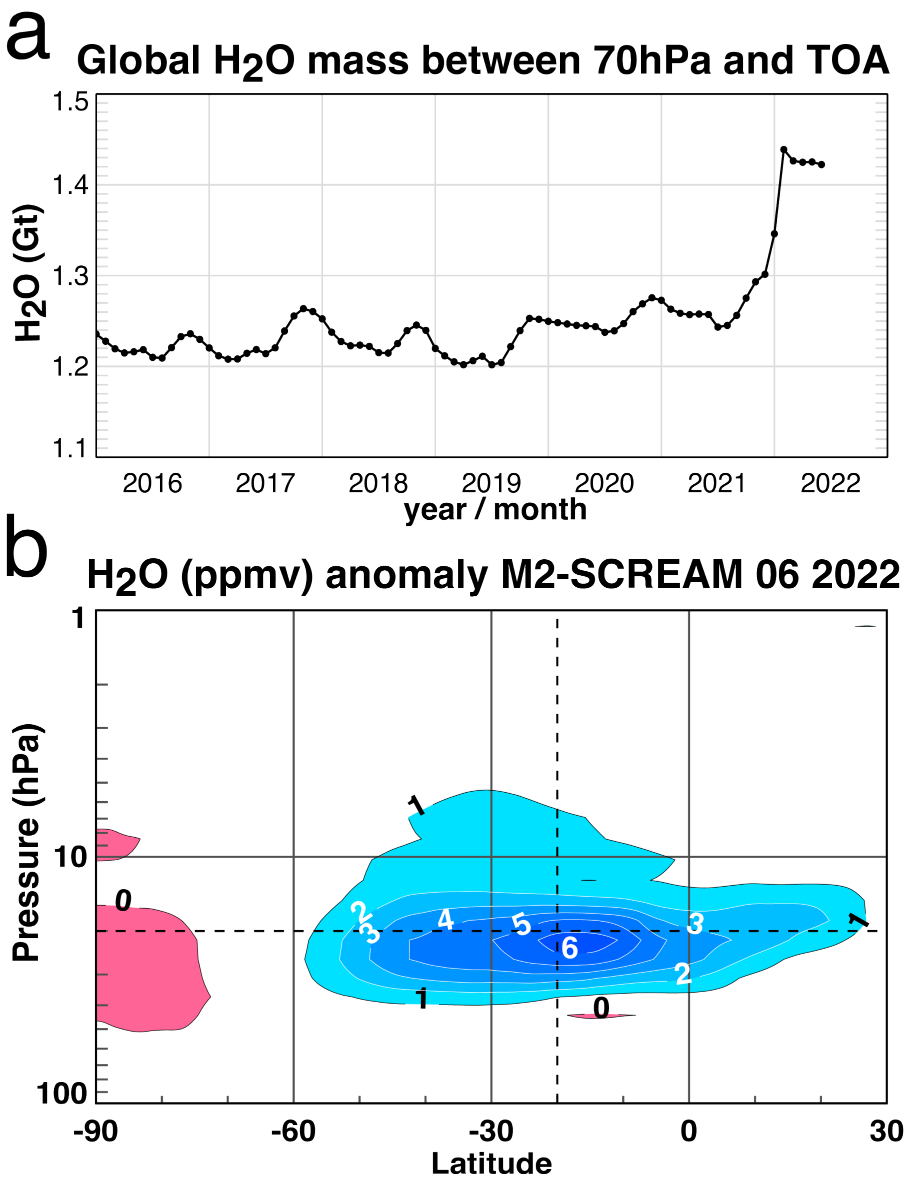

Figure 1: a) Monthly column water vapor mass above 70 hPa as a function of time from M2-SCREAM for the globe, and b) the June 2022 zonally averaged water vapor anomaly (ppmv) from M2-SCREAM as a function of latitude and pressure. The water vapor anomaly is with respect to the 2005 – 2021 M2-SCREAM June average.

3 Results

The assimilation technique in MERRA-2 imposes an additional forcing, the analysis tendency (increments), to force the GEOS model towards the observations. This additional forcing generally manifests as a random error (with a complex spatial and temporal structure), but it can additionally exhibit a mean bias. The latter occurs if some process is not adequately represented by the model. Because the GEOS model uses climatological water vapor fields in the stratosphere of MERRA-2, any anomalous radiative forcing

caused by the volcanic eruption will not be captured in the radiative tendencies and will instead by captured by the bias in the analysis tendency term. The high variability inherent in the analysis temperature tendencies can be reduced by averaging in space and time. The globally averaged analysis temperature tendencies at 20hPa, shown for each month of MERRA-2 (Fig. 2a), reveal the anomalous situation in 2022. Cooling by the analysis increments is progressively stronger than usual, beginning in January. By May 2022 the analysis-induced cooling is over three standard deviations below the mean. These anomalies at 20 hPa coincide with the peak moisture anomaly isolated in Millán et al. (2022) and are the largest in MERRA-2.

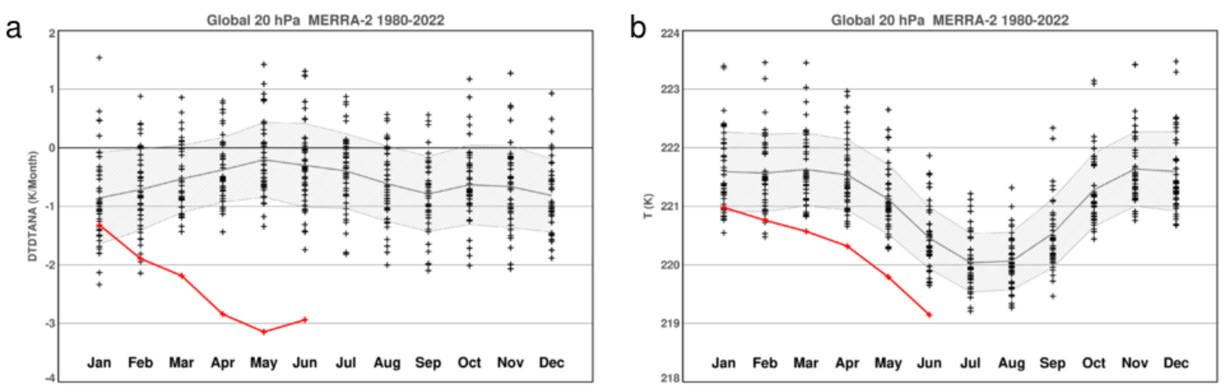

Figure 2: The monthly and globally averaged a) temperature tendencies and b) temperature at 20 hPa. The gray curve denotes the multi-year mean, the gray shading denotes the standard deviation for each month, and the red curve denotes the year 2022.

The analysis increments depict weaker additional cooling at 10hPa and weak additional warming at 30hPa (not shown).

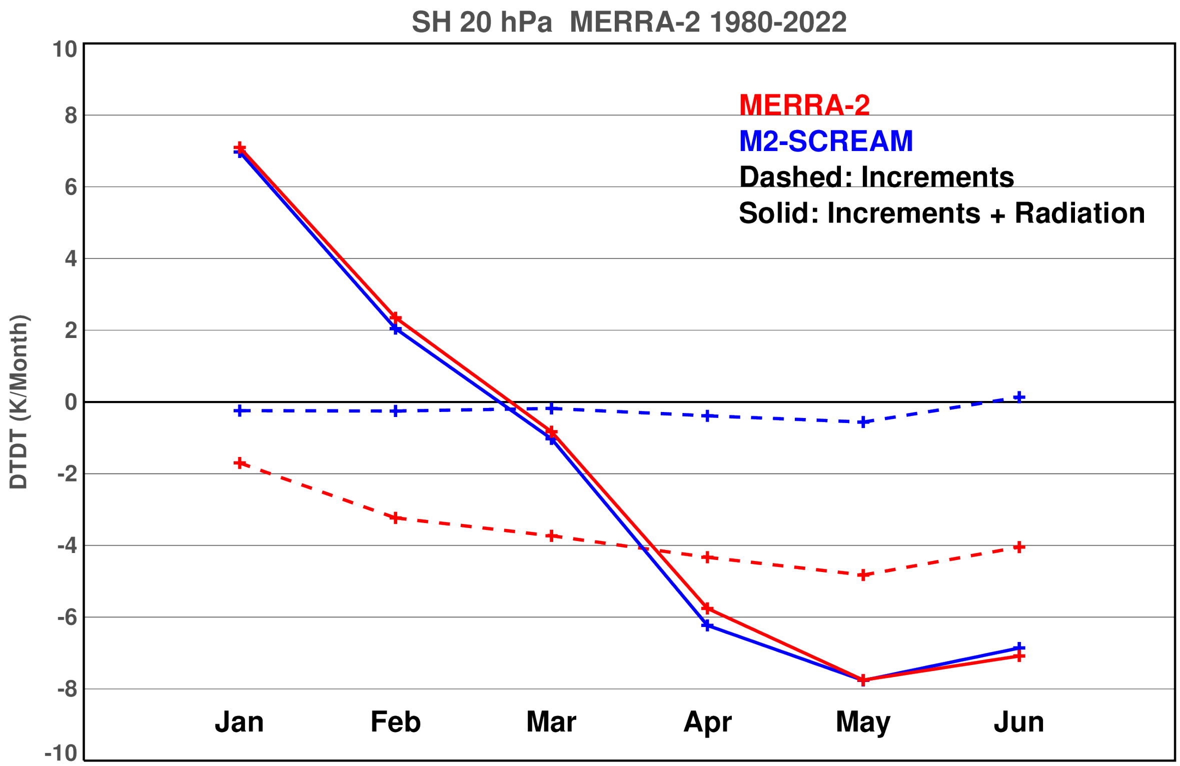

Figure 3: The 20 hPa monthly and Southern Hemisphere averaged MERRA-2 temperature increments (red dashed), MERRA-2 sum of temperature tendencies and radiative tendency (red solid), M2-SCREAM temperature increments (blue dashed), and M2-SCREAM sum of temperature increments and radiative tendency (blue solid).

Between January and June 2022, the global mean temperature at 20 hPa (Fig. 2b) is lower than average values, consistent with the record low analysis. These temperatures are approximately one standard deviation below average in January, continue to decrease in February, and reach their lowest values in the MERRA-2 record between March and June. Note that April through June cools at the same rate as the seasonal cycle, while January through February cools faster than average. Note also that the temperature tendencies can suggest temperatures larger than the temperature departures. For example, in June 2022 the temperature increments are nearly 3 K/month below the mean, while the temperatures for the month are only ~1.25 K below average indicating the importance of the other terms, such as dynamical forcing and radiative transfer, in determining temperature. Nevertheless, these record negative increments are associated with the record low temperatures.

There is further evidence that the anomalous increments correspond to the missing water vapor anomaly in MERRA-2. Figure 3 shows that the M2-SCREAM temperature tendencies averaged over the Southern Hemisphere (SH) have a much smaller magnitude than those in MERRA-2, but that the total (radiation plus analysis increment) tendencies are almost identical. This is because the analyzed water vapor in M2-SCREAM leads to a more realistic computation of radiative cooling, so that the GEOS Model predicts more realistic temperatures that align better to the temperature observations.

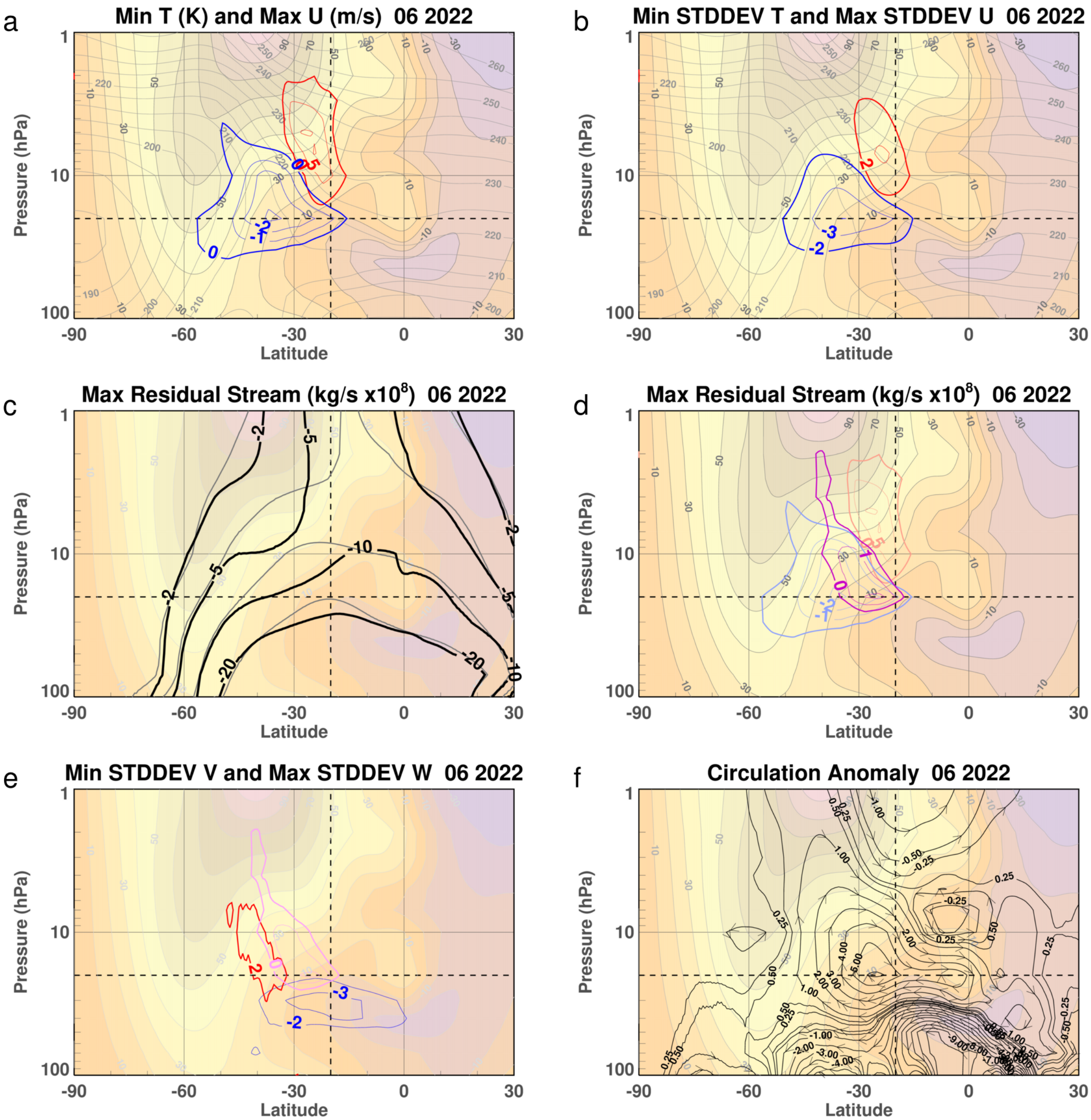

Figure 4: Cross sections for June showing zonal mean zonal winds (10 m/s, filled contours) and temperatures (5K, gray contours (a and b): a) Blue contours: record cold regions where the contours (1 K) denote how much June 2022 is below the previous record low temperature. Red contours: record strong zonal mean winds where the contours (5 m/s) denote how much June 2022 is above the previous record strong wind; b) Blue contours: standard deviations of temperature below the mean (contour interval of 1, starting at -2) and red contours: standard deviations of zonal wind above the mean (contour interval of 1, starting at 2); c) Residual mean stream function (-2, -5, -10, -20 ×10^8 kg/s) for 1980-2021 average (gray) and 2022 (black); d)

residual mean circulation stream function greater than the past maximum value (magenta, contour interval 1×10^8 kg/s) with wind and temperature record as in a); e) Blue contours: standard deviations of residual mean meridional wind below the mean (contour levels of -3 and -2), red contours: standard deviations of residual mean vertical velocity above the mean (contour level of 2) and magenta contours: as in d; f) Difference of the two stream lines shown in c). Dashed lines denote 20ºS and 20 hPa.

This cooling is not uniform over the globe but is strongest near 30°S and 20 hPa. In June 2022 record low temperatures for the month stretch from 55ºS to 15ºS (Fig. 4a). These temperatures break the previous low temperature record by as much 3K. In addition, the zonal mean winds are breaking records by as much as 10 m/s. The location of these record strong winds near the low temperatures is consistent with the geostrophic relation where increased cooling toward the pole requires increased vertical wind shear. In addition to setting records for the month of June, these 2022 low temperatures and strong winds were outside the standard deviation of the year-to-year variability (Fig. 4b) with values greater than double the standard deviation.

These wind and temperature anomalies are likely associated with changes in the mean circulation as the atmosphere adjusts to the temperature perturbation. The counter-clockwise flow of the residual mean stream function for 2022 (Fig. 4c) shows large distortions in the region near the wind and temperature anomalies compared to the 1980-2022 averaged June residual mean stream function. In particular, the strong vertical gradient in the stream function at 30ºS and 30 hPa denotes a stronger that average poleward (negative) flow in 2022. This can be represented as an anomaly in the residual mean stream function (Fig. 4d). In Fig. 4d, the stream function anomaly plotted is greater than any of the previous years in that region. The positive sign of the stream function anomaly denotes a clockwise circulation anomaly. Thus Fig. 4d quantifies the distortion of the stream function from the mean seen in Fig. 4c as being larger than in previous years.

The residual mean circulation can also be expressed in terms of residual mean meridional and vertical velocities (Fig. 4e). The residual mean meridional velocity is particularly striking with negative (poleward) values over three standard deviations below the mean from 10°S-30°S near 30 hPa. The upward mean vertical wind anomalies are over two standard deviations above the mean on the poleward side of the stream function anomaly. This upward anomaly does not correspond to an actual upward circulation but expresses the weaker downward circulation than average as seen in the nearly horizontal stream function regions in Fig. 4c. The residual mean circulation stream function anomaly for June 2022 (Fig. 4f) includes a contribution from the Quasi-Biennial Oscillation (QBO, Baldwin et al., 2001), especially at the equator, however, while the QBO contribution is relatively small by 40°S (not shown), it does reinforce the upward anomaly near 40°S.

4 Conclusions

Anomalous temperatures and circulation patterns analyzed by MERRA-2 in the southern hemisphere during June 2022 can be forensically attributed to the stratospheric water vapor injection from the January 2022 eruption of the Hunga Tonga-Hunga Ha'apai underwater volcano. These anomalies can be traced back to March 2022. Their consistency in space and time suggests a realistic response to a geophysical event rather than a yearly random dynamical fluctuation. In June the 20 hPa record temperature anomaly stretches from 50°S-30°S while the record zonal winds are part of a unusually strong region of the polar vortex centered in the upper stratosphere near 30°S-20°S. In addition, the June mean meridional residual circulation has developed a significant perturbation, slowing descent near ~40°S.

These wind and temperature anomalies (Fig. 4a, b) develop from the assimilation of data, mainly routine, satellite based, nadir viewing radiometers and geostrophic balance and are likely to be very realistic. Note that MERRA-2 does assimilate MLS temperatures, but only at 5 hPa and lower pressures (higher altitudes). The residual mean circulation might be more difficult to interpret. If the cooling analysis temperature increments mainly reflect the missing water vapor cooling then they can be considered to be the missing cooling term from the lack of stratospheric water vapor in the assimilation system. Then the calculated residual circulation (Fig. 4c, d, e) should realistically capture the perturbed residual circulation. If, however, the analysis temperature increments also contain cooling induced by circulations in the atmosphere's response to the water vapor perturbation, then it is possible that the residual circulation may adjust in an unphysical manner. However, the good SH 20 hPa agreement between MERRA-2 and M2-SCREAM seen in the sum of the analysis and radiative temperature tendencies (Fig. 3) suggests that the MERRA-2 analysis tendencies are representative of the missing water vapor cooling. Future work is planned for model simulations that include a realistic representation of the stratospheric water perturbations. These calculations should provide a more complete picture of the atmospheric response to the volcanic perturbation.

Acknowledgments

This work was supported by NASA MAP and ACMAP programs. Resources supporting this work were provided by the NASA High-End Computing (HEC) Program through the NASA Center for Climate Simulation (NCCS) at Goddard Space Flight Center.

Open Research

The MERRA-2 products are available on the NASA Goddard Earth Sciences Data and Information Services Center (GES DISC). Specific MERRA-2 product collections used here are cited appropriately in the references. The 2022 temperature tendencies from M2-SCREAM are available from https://gmao.gsfc.nasa.gov/gmaoftp/STRATOSPHERE/M2-SCREAM/T-tendencies/. Historical M2-SCREAM output can be accessed from https://disc.gsfc.nasa.gov/datasets?keywords=m2-scream&page=1.

References

Andrews, D. G., Holton, J. R., and Leovy, C. B. (1987), Middle Atmosphere Dynamics, Academic Press, 489pp.

Baldwin, M. P., et al. (2001), The quasi-biennial oscillation, *Rev. Geophys.*, 39(2), 179– 229, doi:10.1029/1999RG000073.

Carr, J. L., Horváth, Á., Wu, D. L., & Friberg, M. D. (2022). Stereo plume height and motion retrievals for the record-setting Hunga Tonga-Hunga Ha'apai eruption of 15 January 2022. Geophysical Research Letters, 49, e2022GL098131. https://doi.org/10.1029/2022GL098131

Gelaro, R., McCarty, W., Suárez, M. J., Todling, R., Molod, A., Takacs, L., Randles, C. A., Darmenov, A., Bosilovich, M. G., Reichle, R., Wargan, K., Coy, L., Cullather, R., Draper, C., Akella, S., Buchard, V., Conaty, A., da Silva, A. M., Gu, W., Kim, G., Koster, R., Lucchesi, R., Merkova, D., Nielsen, J. E., Partyka, G., Pawson, S., Putman, W., Rienecker, M., Schubert, S. D., Sienkiewicz, M., & Zhao, B. (2017). The Modern-Era Retrospective Analysis for Research and Applications, Version 2 (MERRA-2), *Journal of Climate*, *30*(14), 5419-5454. Retrieved Jul 27, 2022, from https://journals.ametsoc.org/view/journals/clim/30/14/jcli-d-16-0758.1.xml

Gille, J.C., and L.V. Lyjak (1986). Radiative Heating and Cooling Rates in the Middle Atmosphere. J. Atmos. Sci., 43(20), 2215-2229. DOI: https://doi.org/10.1175/1520-0469(1986)043<2215:RHACRI>2.0.CO;2

Global Modeling and Assimilation Office (GMAO) (2022), M2-SCREAM: 3d,3-Hourly,Instantaneous,Model-Level,Assimilation,Assimilated Constituent Fields,Replayed MERRA-2 Meteorological Fields, Greenbelt, MD, USA, Goddard Earth Sciences Data and Information Services Center (GES DISC), Accessed: July 2022, doi:10.5067/7PR3XRD6Q3NQ

Global Modeling and Assimilation Office (GMAO) (2015a), MERRA-2 instM_3d_asm_Np: 3d,Monthly mean,Instantaneous,Pressure-Level,Assimilation,Assimilated Meteorological Fields V5.12.4, Greenbelt, MD, USA, Goddard Earth Sciences Data and Information Services Center (GES DISC), Accessed: **Jul 27, 2022**, 10.5067/2E096JV59PK7

Global Modeling and Assimilation Office (GMAO) (2015b), MERRA-2 tavgM_3d_tdt_Np: 3d,Monthly mean,Time-Averaged,Pressure-Level,Assimilation,Temperature Tendencies V5.12.4, Greenbelt, MD, USA, Goddard Earth Sciences Data and Information Services Center (GES DISC), Accessed: **Jul 27, 2022**, 10.5067/VILT59HI2MOY

Levelt, P. F., van den Oord, G. H. J., Dobber, M. R., Mälkki, A., Visser, H., Vries, J. D., Stammes, P., Lundell, J. O. V., and Saari, H. (2006). The Ozone Monitoring Instrument, *IEEE Trans. Geosci. Remote Sens*., 44, 1093–1101, https://doi.org/10.1109/TGRS.2006.872333.

Levelt, P. F., Joiner, J., Tamminen, J., Veefkind, J. P., Bhartia, P. K., Stein Zweers, D. C., Duncan, B., et al. (2018). The Ozone Monitoring Instrument: overview of 14 years in space, *Atmos. Chem. Phys*., 18, 5699-5745, https://doi.org/10.5194/acp-18-5699-2018.

Livesey, N. J., Read, W. G., Wagner, P. A., Froidevaux, L., Lambert, A., Manney, G. L. et al. (2020). Version 4.2x Level 2 and 3 data quality and description document, JPL D-33509 Rev. E. Retrieved from https://mls.jpl.nasa.gov/data/v4-2_data_quality_document.pdf, 2020

McCarty, Will, Lawrence Coy, Ronald Gelaro, Albert Huang, Dagmar Merkova, Edmond B. Smith, Meta Seinkiewicz, and Krzysztof Wargan (2016). MERRA-2 Input Observations: Summary and Assessment. NASA Technical Report Series on Global Modeling and Data Assimilation, NASA/TM-2016-104606, Vol. 46, 61 pp. Document (3553 kB).

Millán, L., Santee, M. L., Lambert, A., Livesey, N. J., Werner, F., Schwartz, M. J., et al. (2022). The Hunga Tonga-Hunga Ha'apai Hydration of the Stratosphere. *Geophysical Research Letters*, 49, e2022GL099381. https://doi.org/10.1029/2022GL099381

Schoeberl, M. R., Wang, Y., Ueyama, R., Taha, G., Jensen, E., & Yu, W. (2022). Analysis and impact of the Hunga Tonga-Hunga Ha'apai Stratospheric Water Vapor Plume. *Geophysical Research Letters*, 49, e2022GL100248. https://doi.org/10.1029/2022GL100248

Sellitto P, Podglajen A, Belhadji R, et al. The unexpected radiative impact of the Hunga Tonga eruption of January 15th, 2022. Research Square; 2022. DOI: 10.21203/rs.3.rs-1562573/v1.

Wargan, K., Weir, B., Manney, G. L., Cohn, S. E., K.E. Knowland, P. Wales & Livesey, N. J. (2022). M2-SCREAM: A Stratospheric Composition Reanalysis of Aura MLS data with MERRA-2 transport. Earth and Space Science, submitted. https://www.essoar.org/doi/abs/10.1002/essoar.10512434.1

Wargan, K., Weir, B., Manney, G. L., Cohn, S. E., & Livesey, N. J. (2020). The anomalous 2019 Antarctic ozone hole in the GEOS Constituent Data Assimilation System with MLS observations. *Journal of Geophysical Research: Atmospheres*, 125, e2020JD033335. https://doi.org/10.1029/2020JD033335.

Waters, J. W., Froidevaux, L., Harwood, R.S., Jarnot, R.F., Pickett, H.M., Read, W.G. et al. (2006). The Earth Observing System Microwave Limb Sounder (EOS MLS) on the Aura satellite. *IEEE Trans. Geosci. Remote Sens*., 44, 1075–1092. https://doi.org/10.1109/TGRS.2006.873771.

Xu, J., Li, D., Bai, Z., Tao, M., Bian, J. (2022) Large Amounts of Water Vapor Were Injected into the Stratosphere by the Hunga Tonga–Hunga Ha'apai Volcano Eruption. Atmosphere, 13, 912. https://doi.org/10.3390/atmos13060912.